

Micropower Low-Pass Filter for Medical Electronics Devices Application

WALTER GERMANOVIX
 State University of Londrina
 Department of Electrical Engineering
 Campus Universitário - Londrina - Paraná
 BRAZIL
 w.germanovix@uel.br

Abstract: This work contains a brief study of a new structure of a low-pass filter of N^{th} order, operating in low frequencies. The low-pass filter is designed with CMOS technology and biased to work in weak inversion. The dimension of the lay-out of the circuit and very low power consumption enables this new structure be integrated in a single chip. The parameter n , dependent of the fabrication process, is discussed. Together with the project of the low-pass filter of N^{th} order, this work presents a development of a mathematical tool, including graphs, to design the required characteristic of the filter. Circuit analysis and simulations were performed showing the feasibility of the new structure of low-pass filter proposed. The application of the proposed circuit includes medical electronics devices.

Key-Words: Low-pass filter, Filters in series, Medical Instruments, CMOS, Weak Inversion, Sub-Threshold, Micropower Design.

1 Introduction

There is a need to develop low-power biological amplifiers, which can be integrated in a single chip, capable of processing signals in very low frequencies [2][1]. The present work aims to project a low-pass filter, of order N , tuned to operate in very low frequencies, applicable for medical devices, including electronic prosthesis. This filter has applications in instrumentation amplifiers in order to acquire biological signals with very low frequencies characteristics, as example, the ECG and other biological signals. This circuit is part of major project of a system for acquirement of biological signal in order to process and analyse those signals, as illustrated in the diagram in Fig. 1.

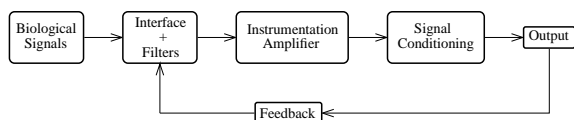


Figure 1: Block diagram showing the acquirement of biological signals. This system has the function to prepare the biological signal for post processing.

There are several requirements in order to project instrumentation amplifier which leads to a simple circuit, with very low power consumption and reduced size, properly indicated for integrated circuit [3]. This

work pursues this way, which in the stage of this project the main concern is to develop a simple N^{th} order low-pass filter, making use of CMOS transistors operating in its sub-threshold region, that is, weak inversion region of operation [10][4]. The core circuit for this project is shown in Fig. 2. This is a CMOS version of a voltage to current converter, named *E+ cell*, inspired from the bipolar technology presented by Frey [6].

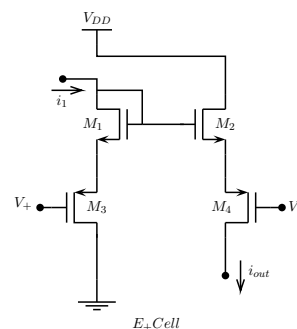


Figure 2: The transconductor *E+ cell* is the main part of the $2gm-C$ filter.

This work presents several results from circuit simulation and a development of mathematical tool together with a graph to specify the *DC* current to tune the low-pass filter of N^{th} order.

2 Projecting the New Low-Pass Filter

The basic circuit of a simple low-pass filter, using the new structure proposed, is shown in Fig. 3.

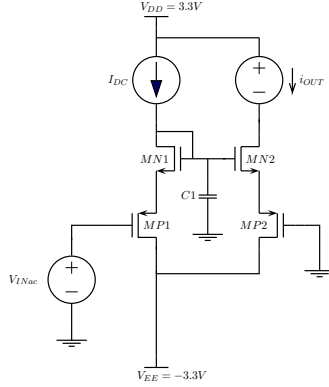


Figure 3: A single pole low-pass filter designed with $2gm$ - C structure.

The function of the $MN1$ and $MP1$ transistors are to act as two transconductance parameters, connected in series. Owing to this kind of connection, the transconductance cell, together with the capacitor $C1$, here is named $2gm$ - C filter. The main function of the $MN2$ and $MP2$ transistors is to furnish the output filtered current.

Through the first order analysis, it is possible to show that the tuning frequency of this low-pass filter is given by (1):

$$\begin{aligned} f_{(-3dB)} &= \frac{1}{2 \cdot \pi \cdot R \cdot C_1} \\ &= \frac{1}{2 \cdot \pi \cdot \left(\frac{1}{g_{m1}} + \frac{1}{g_{m2}} \right) \cdot C_1} \end{aligned} \quad (1)$$

with

$$R = \left(\frac{1}{g_{m1}} + \frac{1}{g_{m2}} \right) \quad (2)$$

where, g_{m1} is the transconductance parameter g_m of the transistor $MN1$ and g_{m2} is the transconductance parameter g_m of the transistor $MP1$ ¹. For the following simulation $I_{DC} = 15nA$, $C1 = 35pF$ and $V_{INac} = 20mV$.

Fig. 4 shows the result of AC analysis, with $-3dB$ frequency, f , equal to $901,2Hz$.

¹For all simulation performed in this work, the process technology considered is *AMS-cmos7tm0_35* model. The dimension of the transistor are $W = 2\mu m$ and $L = 1\mu m$. The power supply applied is $|VCC| = |VEE| = 3.3[V]$ and $V_{SB-Nmos} = V_{BS-Pmos} = 0[V]$. All the graphs were performed making use of MatLab[®] software.

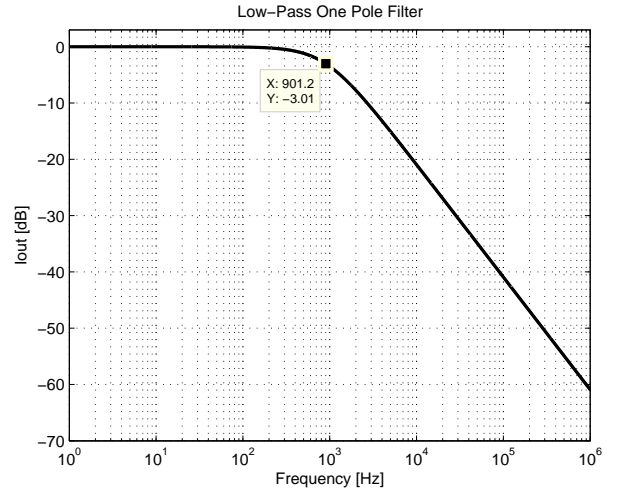


Figure 4: Frequency response of the $2gm$ - C low-pass filter, with single pole. Note that I_{out} is given in (dB). The curve was shifted by $167.6dB$ in order to show the behaviour of the filter from $0dB$. The $-3dB$ frequency is $901,2Hz$.

The $-3dB$ frequency is estimated by (1) and parameters g_m of the $MN1$ and $MP1$ transistors. The transconductance parameters are extracted from the output file provided by spice simulator as indicated below:

Table 1: Extracted Parameters from Spice

Transistor	$MN1$ -Nmos	$MP1$ -Pmos
g_m	$4.15E-07$	$3.78E-07$

$$g_{m1} = g_{mMN1} = 4.15 \times 10^{-7} [S] \quad (3)$$

and

$$g_{m2} = g_{mMP1} = 3.78 \times 10^{-7} [S] \quad (4)$$

Applying (1), with the data above, the result is $899,54Hz$, which is quite close to the result of the simulator ($901,2Hz$), as shown in Fig. 4.

3 The parameters g_m and g_{ds}

As the transistor of the filters are operating in weak inversion, g_m and g_{ds} are controlled by polarization current, I_{DC} , so this filter, can be tuned by current, according to the following relationship [10] [5]:

$$g_m = \frac{I_o}{n \cdot \phi_t} \quad (5)$$

$$g_{ds} = \frac{I_o}{|V_A|} \quad (6)$$

where I_o is constant current, represented in Fig. 3 by I_{DC} , ϕ_t is the *thermal voltage* and n is a process dependent of fabrication. The parameter V_A is similar to the Early voltage comparable with bipolar technology. So, in function of current I_o and parameters of the transistors, (1) is written as:

$$f_{(-3dB)} = \frac{I_0}{2 \cdot \pi \cdot \left(\frac{n_N \cdot \phi_t \cdot |V_A|_N}{n_N \cdot \phi_t + |V_A|_N} + \frac{n_P \cdot \phi_t \cdot |V_A|_P}{n_P \cdot \phi_t + |V_A|_P} \right) \cdot C_1} \quad (7)$$

where n_N and n_P are the n parameter dependent from the process technology, for NMOS and PMOS transistors respectively. The parameter $|V_A|_N$ and $|V_A|_P$ are $|V_A|$ values for NMOS and PMOS respectively. Considering $(n_N \cdot \phi_t + |V_A|_N) \cong |V_A|_N$ and $(n_P \cdot \phi_t + |V_A|_P) \cong |V_A|_P$ (7) is simplified to:

$$f_{(-3dB)} = \frac{I_0}{2 \cdot \pi \cdot \phi_t (n_N + n_P) \cdot C_1} \quad (8)$$

This confirms that the frequency, of the proposed filter, can be adjustable by polarization current I_o .

3.1 The Parameter n

Unfortunately the n parameters, here represented as n_N and n_P , varies slightly with V_{GS} voltage of the transistor CMOS. In this case it is convenient extract the dependence of the n parameters, in relation to variation of V_{GS} (or I_{DC}), for both types of transistors. From the data provided by Spice simulator and (5) was extracted two curves, showing the dependence of n , in respect to the current I_o , for the NMOS and PMOS transistors, designed from a particular technology.

Fig. 5 show, the variation of n , according to variation of the current I_o , for the NMOS and PMOS transistors.

Looking to the simulation, shown in Fig. 4, the $-3dB$ frequency for the filter of Fig. 3, is $f_{(-3dB)} = 901,2Hz$, when applied $I_{DC} = 15nA$ and $C = 35pF$. Applying (8) for $I_o = 15nA$, and extracting n_N and n_P from Fig. 5, on which are found $n_N = 1.383$ and $n_P = 1.527$, the $-3dB$ frequency is calculated equal to $906,68Hz$, which is close to the simulation. Recall that (8) is an approximation of the complete (7), showing that the model proposed is a good approximation.

4 Improving the Low-Pass Filter

The principle of functioning of the proposed filter is the same as gm - C filter [9]. The new filter structure

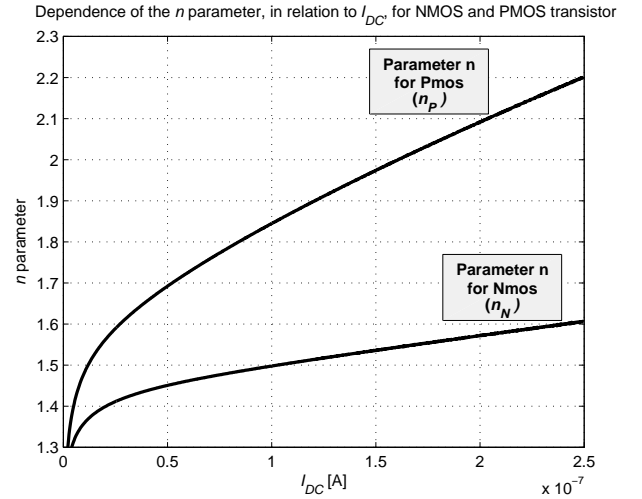


Figure 5: Relating to (5), here I_o is symbolized by I_{DC} . From this plot it is possible to extract the dependence of n in relation to I_{DC} . As example, variation of the parameter n according to variation of the current I_o through the NMOS transistor: $n = 1.383$ for $I_{DC} = 15nA$; $n = 1.422$ for $I_{DC} = 30nA$; $n = 1.462$ for $I_{DC} = 60nA$; $n = 1.514$ for $I_{DC} = 120nA$. And, variation of the parameter n according to variation of the current I_o , through the PMOS transistor: $n = 1.527$ for $I_{DC} = 15nA$; $n = 1.613$ for $I_{DC} = 30nA$; $n = 1.726$ for $I_{DC} = 60nA$; $n = 1.898$ for $I_{DC} = 120nA$.

shown on Fig. 3 has two cascaded transistors, with advantage that the voltage signal can be applied direct into the input of the filter (gate of MPI) and, the resulting electrical current can be conditioned or processed. The input voltage source, V_{INac} , can be a biological signal, with very low incremental voltage and very low frequency, which is directly applied to the input of the filter. One another advantage of this structure is the sum of two transconductances parameters. This effect increases the time constant, applicable where is required very low frequencies. This characteristic makes possible to integrate, in a single chip, all the components of the circuit. Looking into the circuit, presented in Fig. 3, the disadvantage is the variation of current source, I_{DC} , responsible for tuning of the filter, meaning that the tuning current implies in changing the amplitude of the output signal. In this point of view, the circuit has to be improved, in order to keep the average output current constant, even varying I_{DC} in order to tune the frequency response of the filter.

Fig. 6 shows the improved version of the simple low-pass filter, with two additional advantages, the

tuning current do not modify the amplitude of the output current and one more pole is added.

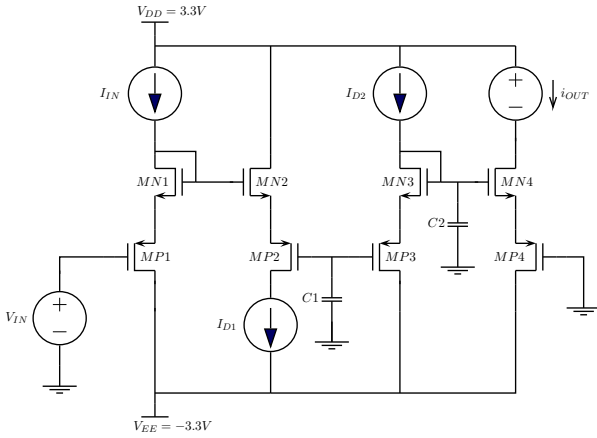


Figure 6: Two gm-C cells in series, acting as two poles low-pass filter.

Referring to the circuit shown in Fig. 6, the function of transistors MP1 and MN1, together with I_{IN} is to provide the input to the filter (gate of MP1). The input of the filter is in form of voltage signal. The function of the transistors MP2 and MN2, together with I_{D1} , is to provide two gm's in series, in order to combine with C1 capacitor, forming the first cell RC. The function of the transistors MP3 and MN3, together with I_{D2} , is to provide two gm's in series, in order to combine with C2 capacitor, forming the second cell RC. The function of the transistors MP4 and MN4 is to provide the output signal, in form of filtered current.

5 Block Diagram for Low-Pass Filter

In order to understand the behaviour of the filter with two (or N) cells, in the same way as a connection of RC filter in series, is presented a brief revision of the Nth order filter, as shown in Fig. 7 and Fig. 8. Here $R = (1/g_1 + 1/g_2)$, is component of (1).

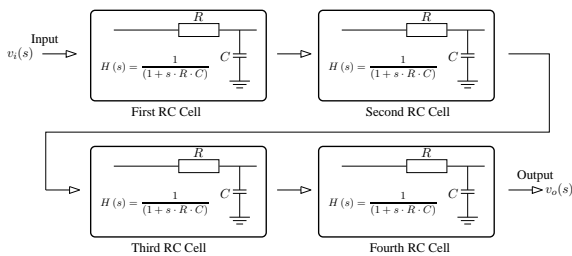


Figure 7: Four RC low-pass filters in series.

Fig. 7, represents four low-pass filters connected in series where, each of them has the following transfer function:

$$H(s) = \frac{1}{1 + s \cdot R \cdot C} \tag{9}$$

The Bode Diagrams in Fig. 8 illustrates the response frequency of the input voltage signal and the respective output for each RC cell.

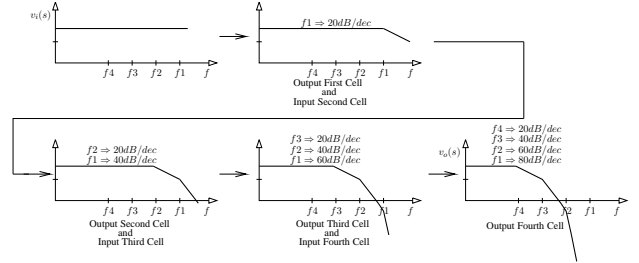


Figure 8: This illustration shows how the corner frequency (-3dB) of the first cell is attenuated additionally in -3dB, each time it enters in the next stage.

Note that, in the output of the first cell, the -3dB frequency, f_1 , is applied to the input of the second cell. So, in the output of the second cell, f_1 is attenuated more -3dB, giving place to a new frequency, f_2 , with -3dB of attenuation. Now, in the output of the third cell, f_2 is attenuated additionally -3dB, giving place to the frequency f_3 attenuated in -3dB (related to f_2). The fourth cell, provides the corner frequency, f_4 , again attenuated by -3dB. So, from f_4 the input signal was attenuated 20dB/dec, from f_3 by 40dB/dec, from f_2 by 60dB/dec and from f_1 the signal is attenuated by 80dB/dec. This idea is applied to filters with Nth order.

The transfer function of the structure, shown in Fig. 7, is:

$$H(s) = \frac{v_0(s)}{v_i(s)} = \left(\frac{1}{1 + s \cdot R \cdot C} \right)^N = \frac{\left(\frac{1}{R \cdot C} \right)^N}{\left(s + \frac{1}{R \cdot C} \right)^N} \tag{10}$$

where N is the number of cells RC connected in series. Using an auxiliary constant, $K = 1/(R \cdot C)$, (10) can be written as:

$$H(s) = \frac{(K)^N}{(s + K)^N} \tag{11}$$

and substituting, $s = j \cdot \omega$, where j is the complex number and ω is the variable frequency, it results:

$$H(j\omega) = \frac{(K)^N}{(j \cdot \omega + K)^N} \tag{12}$$

Extracting the absolute value from this function:

$$\begin{aligned}
 H &= |H(j\omega)| = \left| \frac{(K)^N}{(j \cdot \omega + K)^N} \right| \\
 &= \frac{K^N}{(\sqrt{\omega^2 + K^2})^N} = \frac{K^N}{(\omega^2 + K^2)^{\frac{N}{2}}} \quad (13)
 \end{aligned}$$

The modulus of the transfer function shows the amplitude of the output signal, H , in function of the frequency ω . Supposing that it is desirable calculate the frequency in function of the absolute value, H . In this case, isolating ω from (13) it results:

$$\omega = K \cdot \sqrt{\frac{1}{H^{\frac{2}{N}}} - 1} \quad (14)$$

(14) allows to calculate the frequency, according to the N numbers of cells in series, which is $3,01dB$ below its absolute value. In such case (14) is rewritten as:

$$f_{(-3dB)} = \frac{K}{2 \cdot \pi} \cdot \sqrt{2^{\frac{1}{N}} - 1} \quad (15)$$

6 Filter with Four Cells in Series

Using the same process of fabrication and data from the filter cell presented in Fig. 3, together with (3) and (4), on which $R = (1/g_1 + 1/g_2) = 5.04M\Omega$, $C = 35pF$, and calculating frequencies responses from (15), as example, a filter compound by four $2gm-C$ cells filter, so N varies from 1 to 4, it results respectively: $f_1 = 901,12Hz$; $f_2 = 579,96Hz$; $f_3 = 459,41Hz$; and $f_4 = 391,97Hz$.

Fig. 9 shows an implementation of a low-pass filter compounded by four $2gm-C$ cells in series ($N=4$).

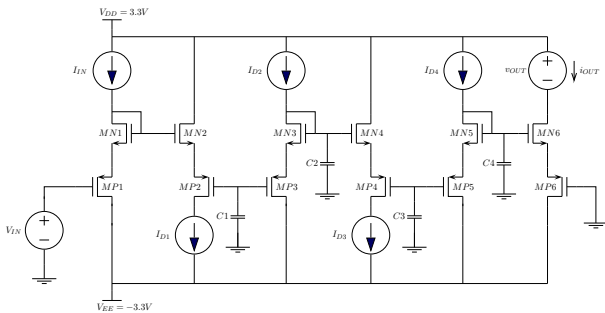


Figure 9: Four $2gm-C$ cells in series resulting a low-pass fourth order filter.

The simulation in Fig. 10 shows the results for respectively four filter, that is, from $N = 1$ to $N = 4$.

The frequency that occurs $-3.01dB$ attenuation are: $f_1 = 902Hz$, $f_2 = 580Hz$, $f_3 = 459Hz$ and, $f_4 = 392Hz$, very well comparable, with mathematical prediction shown in (15).

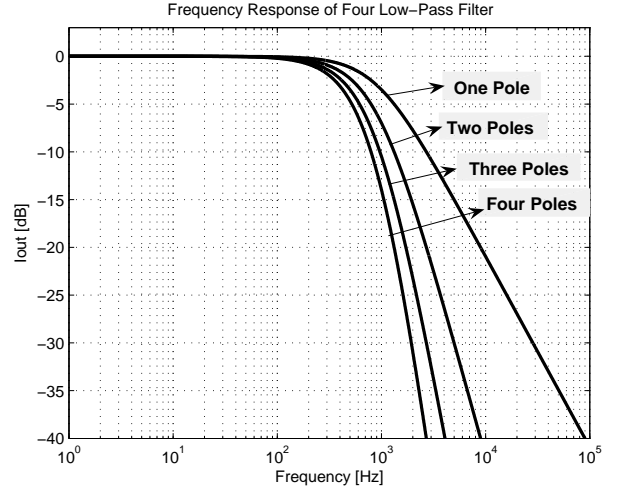


Figure 10: Simulation results for low-pass filters. The N order of the filter varies from 1 (first order) to 4 (fourth order).

7 Designing N Cells in Series

Applying the concepts described in Sub-Section 3.1 a new method is proposed in this work to design a N^{th} order, with $2gm-C$ cells in series. The problem consist in furnish the required frequency attenuated by $-3dB$, how many cells in series are necessary and finally calculate which is the I_{DC} current in order to tune this $2gm-C$ filter.

Expanding (5) for the proposed $2-gm$ cell it results:

$$(g_{m1} + g_{m2}) = \frac{I_{DC}}{(n_N + n_P) \cdot \phi_t} \quad (16)$$

Isolating I_{DC}

$$I_{DC} = \frac{\phi_t \cdot (n_N + n_P)}{\left(\frac{1}{g_{m1}} + \frac{1}{g_{m2}}\right)} \quad (17)$$

Recall that the auxiliary constant K in (15) is $K = 1/(R \cdot C)$ and from (2)

$$R = \left(\frac{1}{g_{m1}} + \frac{1}{g_{m2}}\right)$$

Now, (17) can be rewritten as:

$$\frac{1}{R} = \frac{I_{DC}}{\phi_t \cdot (n_N + n_P)} \quad (18)$$

(18) is a key to plot a function

$$f(I_{DC}) = \frac{I_{DC}}{\phi_t \cdot (n_N + n_P)} \quad (19)$$

as shown in Fig. 11

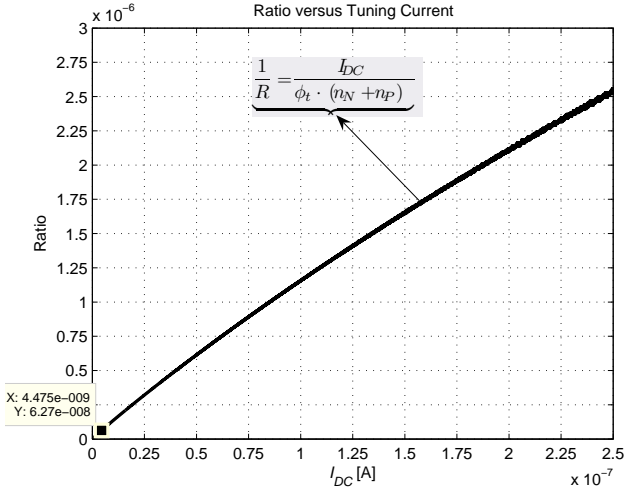


Figure 11: Variation of the tuning current I_{DC} with calculated $1/R$.

As example: $N=8$ (eight cells in series), $-3.01dB$ of attenuation in the frequency $200Hz$ is specified and $C=15pF$ is adopted. From (15)

$$200 = \frac{1}{2 \cdot \pi \cdot R \cdot 15p} \cdot \sqrt{2^{1/8} - 1} \quad (20)$$

it results

$$R = 15.96M\Omega \quad (21)$$

Preparing the value of R in (18), it results $1/R = 6.265 \times 10^{-8}$. Taking this value and with the data presented in Fig. 11 it is found $I_{DC} = 4.47n[A]$. This results means that, for the example proposed, the filter compound by eight $2gm-C$ cells, connected in series, with $200Hz$ attenuated by $-3dB$, is necessary to bias each cell with $I_{DC} = 4.47n[A]$.

Fig. 12 shows the implementation of the circuit with its input, output and eight cells in series.

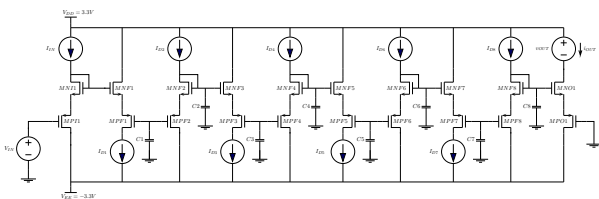


Figure 12: Eighth order low-pass filter, that is, $N = 8$, resulting in $-160dB/decade$ of attenuation.

The transistors $MN11$ and $MP11$, together with the current source, I_{IN} , are the input of the circuit. Applying the translinear principle [7] [8], the steady current in $MNO1$ and $MPO1$, I_{OUT} , is provided by the transistors $MN11$ and $MP11$. The incremental output signal (current i_{out}) is added to the steady current (DC) giving an excursion of the output signal in form of current. Transistors MNF_i and MPF_i , together with the source of current for tuning the frequency, I_{D_i} , for $i = 1$ to 8 , are eight $2gm-C$ cells in series. Transistors $MNO1$ and $MPO1$ provide the output current of the circuit.

Fig. 13 shows the simulation of the eight $2gm-C$ cells in series, according to Fig. 12. The frequency required was $200Hz$ and the circuit provided about $199.7Hz$, meaning that the first order analysis, provided by Fig. 11, is very close to the simulation.

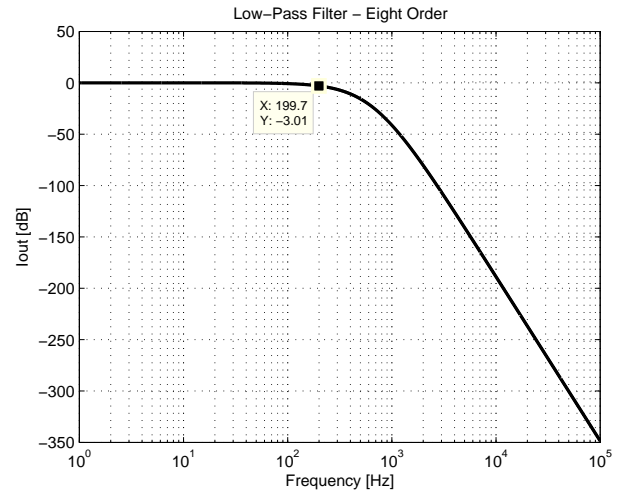


Figure 13: This simulation shows a low-pass filter with eighth order. The corner frequency is $f_{(-3dB)} = 199.7Hz$.

8 Additional Simulation Analysis

The current sources, I_{D1} to I_{D4} , of the circuit presented in Fig. 9 were replaced by actual current source. A good choice of a current source is the advanced wide-swing cascode current-mirror, with enhanced output impedance. For this particular study, a simple cascode current-mirror was chosen, as shown in Fig. 14.

It was performed three types of simulations: the transient analysis, DC and temperature variation. The current source I_B was set to $15n[A]$ in order to tune the filter in $392Hz$, the current source I_{IN} was set to $150n[A]$ and the voltage source V_{IN} provides a sinusoidal signal with $20m[V_{pp}]$.

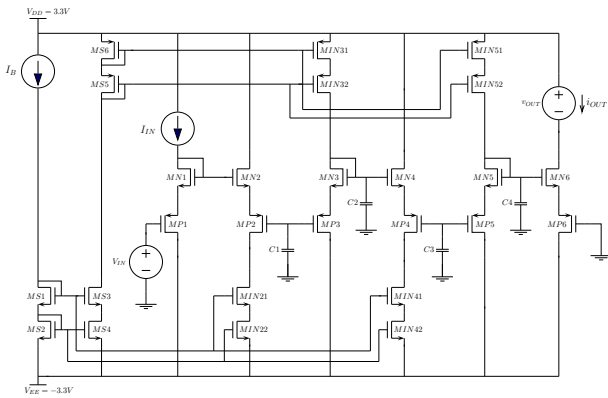


Figure 14: The simple cascode current-mirror replaces the ideal current sources of $2gm-C$ filters.

8.1 Transient Analysis

The four poles low-pass filter was tuned at $f_{(-3dB)} = 392Hz$. The simulation is shown in Fig. 15.

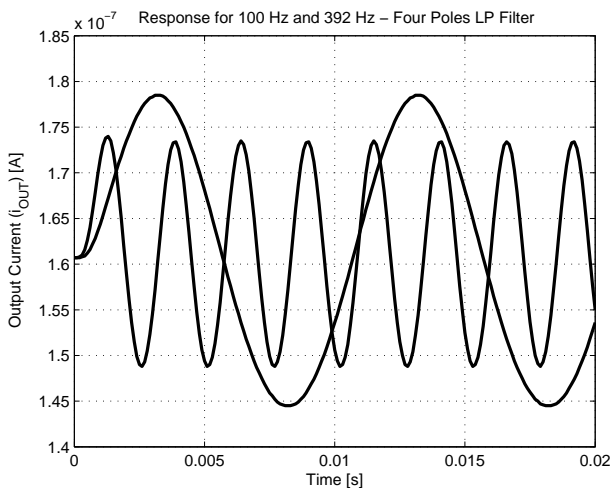


Figure 15: Transient Analysis for Four Poles Low-Pass Filter. The corner frequency is $f_{(-3dB)} = 392Hz$.

The simulation result shows that the signal with $f = 392Hz$ is attenuated by $-3dB$ related to the signal with $f = 100Hz$. This means the result is comparable with the result of AC analysis, shown in Fig. 10.

8.2 DC Analysis

In the input of the transconductor circuit (V_{IN}), Fig. 14, was applied a voltage ranging from $-100mV$ to $+100mV$. The output current was plotted as shown in Fig. 16.

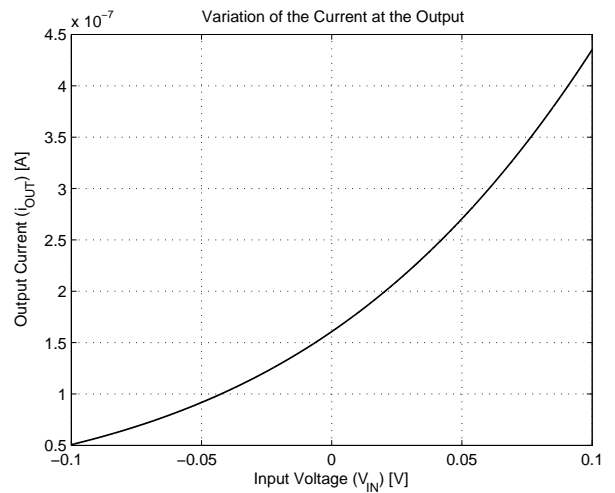


Figure 16: DC Analysis for the Transconductor Circuit.

As expected, the variation of the input signal has to obey the principle of small signal analysis [5]. This means, in order to keep linearity of the transconductor, this circuit is only applied for small signals which is the case of electrical biological signals.

8.3 Temperature Variation Analysis

The same DC analysis was performed with temperatures equal to $0^{\circ}C$, $27^{\circ}C$ and $75^{\circ}C$. The results are shown in Fig. 17.

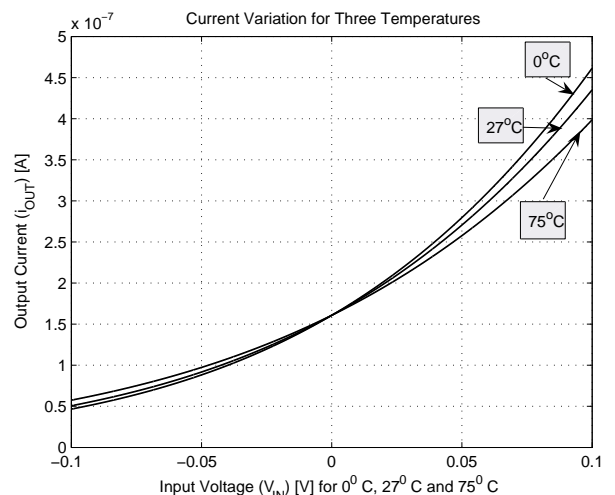


Figure 17: For this DC analysis temperatures were set to $0^{\circ}C$, $27^{\circ}C$ and $75^{\circ}C$.

It can be observed that, even with a large variation of temperature, there are a little variation in the output current, i_{OUT} . This is due to the translinear

principle where CMOS transistor, operating in weak inversion, has similar drain current equation related to the collector current equation in bipolar technology.

9 Conclusion

A micropower low-pass filter was presented. The steps shown in this work are pointed out to the development of a new structure of low-pass filter making use of transconductance cells. The design is based on CMOS technology, resulting into two important characteristics, properly for integrable filter in a single chip: lay-out with reduced area, even for operation in low frequencies and micropower consumption of energy, since that, the CMOS transistors are polarized to work in weak inversion (sub-threshold region of operation). The transconductance cell are formed by two cascaded transistor, PMOS and NMOS. The respective transconductance parameters of each transistors are connected in series and owing to this type of the connection, here the cell was named $2gm-C$. It was presented the project of the filter with one pole, four poles and eight poles. The main advantage of this type of circuit structure is the easy tuning of the corner frequency. Mathematical tools were developed in order to show how to specify the DC current in order to polarize the cells that compound the filter. Another important analysis was in respect to parameter n , dependent of the process of fabrication. It was verified that this parameter varies slightly with the current of polarization of the CMOS transistor. Finally, it was shown an auxiliary graph to help to verify the current in order to tune the filter. The field of Medical Electronics is an example of application of this kind of filters. Simulation results and the mathematical tool developed in this work show that these filters are candidate to become part of systems on which are required very low frequency of operation and very low power consumption. Next step will be the integration of the proposed filter in a single chip.

Acknowledgements: This research is supported by the State University of Londrina - Parana - Brazil.

References:

- [1] Christopher D. Salthouse and Rahul Sarpeshkar, A Practical Micropower Programmable Band-pass Filter for Use in Bionic Ears, *IEEE Journal of Solid-State Circuits* 38(1), 2003, pp. 63–70.
- [2] Reid R. Harrison and Cameron Charles, A Low-Power Low-Noise CMOS Amplifier for Neural Recording Applications, *IEEE Journal of Solid-State Circuits* 38(6), 2003, pp. 958–965.
- [3] W. Germanovix and C. Toumazou, Design of a Micropower Current-Mode Log-Domain Analog Cochlear Implant, *IEEE Transactions on Circuits and Systems-II: Analog and Digital Signal Processing* 47(10), 2000, pp. 1023–1046.
- [4] E. A. Vittoz and J. Fellrath, CMOS analog integrated circuits based on weak inversion operation, *IEEE Journal of Solid-State Circuits* 12, 1977, pp. 224–231.
- [5] Paul R. Gray, Paul J. Hurst, Stephen H. Lewis and Robert G. Meyer, *Analysis and Design of Analog Integrated Circuits*, John Wiley & Sons, Inc. 2001
- [6] Douglas R. Frey, Exponential State Space Filters: A Generic Current Mode Design Strategy, *IEEE Transactions on Circuits and Systems-I: Fundamental Theory and Applications* 43(1), 1996, pp. 34–42.
- [7] B. Gilbert, Translinear Circuits: A proposed Classification, *Electronics Letters* 11(1), 1975, pp. 14–16.
- [8] Evert Seevinck and Remco J. Wiegerink, Generalized Translinear Circuit Principle, *IEEE Journal of Solid-State Circuits* 26(8), 1991, pp. 1098–1102.
- [9] Yannis Tsividis, Integrated Continuous-Time Filter Design - An Overview, *IEEE Journal of Solid-State Circuits* 29(3), 1994, pp. 166–176.
- [10] Yannis Tsividis, *Mixed Analog-Digital VLSI Devices and Technology*, McGraw Hill 1995